Predrag Milić
Dragan Marinković

ISSN 1333-1124
eISSN 1849-1391

ISOGEOMETRIC FE ANALYSIS OF COMPLEX THIN-WALLED STRUCTURES

Summary

Isogeometric analysis, as a special field of the finite element method (FEM) which integrates geometric and finite element mesh modelling, is one of the promising directions of FEM development. The paper presents a concept of isogeometric FEM analysis of thin-walled structures based on the Kirchhoff-Love shell formulation and NURBS as basis functions. The basic properties of isogeometric shell model are briefly given by means of NURBS interpolation functions. The problem of setting up larger models that involve multiple patches and their interconnection is addressed. Academic models as well as practical models from the field of heavy construction equipment demonstrate the applicability of developed tools for static FEM analysis.

Key words: *Isogeometric analysis, FEM, NURBS, Kirchhoff-Love shell*

1. Introduction

Isogeometric analysis, first introduced by Hughes et al. [1], represents a special approach adopted in the finite element method (FEM) which aims at closing the gap between the actual geometry of modelled structures and the geometry generated by means of the finite element discretization. In the classical FE formulations for structural analysis, the isoparametric approach is favoured. It implies the use of mainly linear and quadratic Lagrange polynomials as element shape functions that describe both the displacement field and geometry. As a consequence, the geometry of the FEM model is only an approximation of the actual geometry and the quality of approximation depends on the mesh density. On the other hand, in the framework of isogeometric FE analysis, NURBS (non-uniform rational basis spline) functions form the basis for the definition of both the geometric models and interpolation functions of FE models. Regardless of the mesh density, the geometry is exactly described in the FEM model, hence the characterization ‘isogeometric’.

Roughly speaking, up to 80% of the structures the engineers deal with in practice belong to the group of thin-walled structures with the slenderness ratio (in-plane dimensions-to-thickness ratio) higher than 10. The typical approach to their FEM modelling implies condensation of the 3D-field to a 2D one. A distinction is made between two basic first-order 2D theories. The Kirchhoff-Love theory [2] neglects the transverse shear effects, which makes the theory suitable for the natural structural response of rather thin structures

(slenderness ratio higher than 20 with isotropic materials and even higher than 100 with composite laminates). The Mindlin-Reissner theory, on the other hand, accounts for the transverse shear effects in a simplified manner, which makes it suitable for thicker shell structures [3]. Despite those basic differences, both theories are supposed to yield the same response for thin structures. However, meeting this condition in the framework of classical FEM turns out not to be such a trivial task. Namely, in the classical FEM, the Mindlin-Reissner shell formulation yielded a number of workhorse elements for thin-walled structures (e.g. [4, 5, 6, 7]) due to the fact that it requires only the C^0-continuity from the shape functions (e.g. Lagrange polynomials), whereas the Kirchhoff-Love formulation demands the C^1-continuity over the element boundaries. But it is the combination of Lagrange polynomials as shape functions, the isoparametric approach and the definition of the constrained strain field (for thin structures, no transverse shear effects and no membrane effects at pure bending) that gives rise to the well-known problems of shear and membrane locking with Mindlin-Reissner shell elements. A number of remedies have been used so far [8, 9], which are however not derivatives of the variational approach. This puts a question mark over the reliability of obtained results.

NURBS as a type of spline is not only suitable for the description of complex geometric forms, but its level of continuity can also be easily set to meet specific application demands. Hence, after the development of a NURBS-based FEM for solids [10], the authors put focus in this paper on the formulation of a NURBS-based Kirchhoff-Love shell element for modelling thin-walled structures together with a technique for generating complex models as an assembly of coupled patches.

2. B-spline and NURBS basic functions

Geometric and FEM models based on NURBS surfaces are in the focus of this paper. As these functions have a significant influence on the considered model properties, a brief overview of the basis spline (B-spline) and NURBS functions, curves, and surfaces is given below.

The advantage of NURBS in relation to a B-spline is reflected in the possibility of accurate descriptions of complex geometric shapes. Although NURBS differs from B-spline, it actually uses B-splines as basic functions, as the name reveals.

A B-spline of the order p given for the knot vector $\Xi=[\xi_0, \xi_1, ..., \xi_{n+p+1}]$ is determined by the Cox-De Boor recursive formula [11]. For the degree $p = 0$, the basic functions are determined as:

$$N_{i,0}(\xi)=\begin{cases}1 & \xi_i \le \xi < \xi_{i+1} \\ 0 & \text{otherwise}\end{cases}. \tag{1}$$

Basic functions of the order greater than zero are given as:

$$N_{i,p}(\xi)=\frac{\xi-\xi_i}{\xi_{i+p}-\xi_i}N_{i,p-1}(\xi)+\frac{\xi_{i+p+1}-\xi}{\xi_{i+p+1}-\xi_{i+1}}N_{i+1,p-1}(\xi). \tag{2}$$

The knot vector is a set of parametric coordinates ξ_i in a non-decreasing order. The continuity of basis functions depends on the function order, p, and knot multiplicity. At the knot multiplicity k the continuity is C^{p-k}. Some important characteristics of these basic functions are: $N_{i,0}(\xi)$ is a stepped function equal to zero for all ξ except for half open interval $\xi \in [\xi_i, \xi_{i+1})$; $N_{i,p}(\xi)$ is a linear combination of two functions of the degree (p-1); a basic

function of the order p has a value different from zero only in the semi-interval $\xi\in[\xi_i, \xi_{i+p+1})$; sum of all basic functions of the order p at a point ξ equals one (partition of unity); they are non-negative and linearly independent.

A p-order NURBS curve can be represented as a rational function using B-spline basic functions by means of the following expression [1, 12, 13]:

$$C(\xi)=\frac{\sum_{i=0}^{n} N_{i,p}(\xi)w_i P_i}{\sum_{i=0}^{n} N_{i,p}(\xi)w_i}=\sum_{i=0}^{n} R_{i,p}(\xi)P_i \quad a\le\xi\le b, \tag{3}$$

where P_i are the control points that form a control polygon, w_i are the weights, $\{N_{i,p}(\xi)\}$ are the B-spline basic functions of the order p defined on the non-uniform knot vector $\Xi=\{a,...,a,\xi_{p+1},..., \xi_{m-p-1}, b,...,b\}$, while $R_{i,p}$ are the p-order basic rational functions of the NURBS.

Usually, the knot vector is normalized, i.e. $a = 0$ and $b = 1$. Repetition of the elements a and b in the knot vector depends on the order of spline and it is p+1. In this way, the discontinuity is realized at the ends of the spline. A NURBS surface of the order p in the ξ-direction and the order q in the η-direction can be expressed as:

$$S(\xi,\eta)=\frac{\sum_{i=0}^{n}\sum_{j=0}^{m} N_{i,p}(\xi)N_{j,q}(\eta)w_{ij}P_{ij}}{\sum_{k=0}^{n}\sum_{l=0}^{m} N_{k,p}(\xi)N_{l,q}(\eta)w_{k,l}} \quad 0\le\xi,\eta\le 1. \tag{4}$$

By substituting the basic rational function:

$$R_{ij}(\xi,\eta)=\frac{N_{i,p}(\xi)N_{j,q}(\eta)w_{ij}}{\sum_{k=0}^{n}\sum_{l=0}^{m} N_{k,p}(\xi)N_{l,q}(\eta)w_{kl}} \quad 0\le\xi,\eta\le 1, \tag{5}$$

the equation for the surface takes the form:

$$S(\xi,\eta)=\sum_{i=0}^{n}\sum_{j=0}^{m} R_{ij}(\xi,\eta)P_{ij} \quad 0\le\xi,\eta\le 1. \tag{6}$$

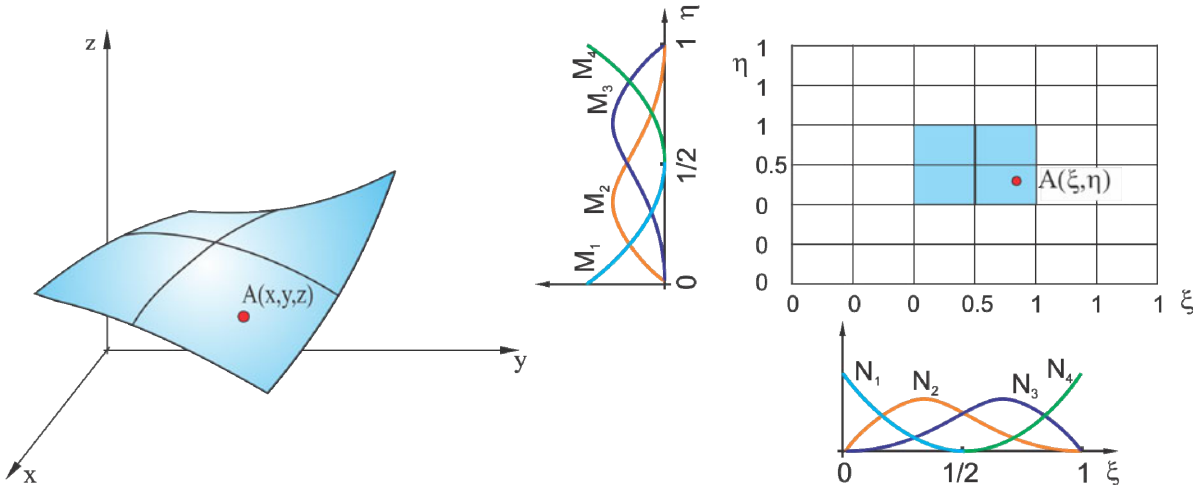

Fig. 1 An example of NURBS surfaces with quadratic basic functions

3. Kirchhoff-Love shell kinematics and finite element formulation

In 1850, Kirchhoff [14] introduced a hypothesis on the behaviour of elastic plate deformation that represents an extension of the Euler-Bernoulli beam theory. The hypothesis assumes that a straight line normal to the mid-surface of the undeformed structure remains straight, perpendicular to the mid-surface, and unstrained after deformation. This theory has been extended to curved thin-walled structures by Love [15].

As already mentioned, this theory is suitable for rather thin shells, i.e. structures with high slenderness ratio. Because of the presence of the second order derivative of the approximation function in the expression for the virtual work, Kirchhoff's elements require the C^1-continuity across the element boundaries, which is physically interpreted as the continuity of rotations. The NURBS surface resolves this problem as it provides the continuity of basic functions throughout multiple elements, thus offering at least the C^1-continuity. However, complex surfaces need to be modelled as an assemblage of patches, where each single patch is defined as a NURBS surface. The C^1-continuity between patches is not given *per se*, thus requiring an adequate solution, as it will be elaborated later.

The shell element kinematics and the formulation that is only briefly presented below follow the development presented by Nguyen et al. [16], which is a total Lagrangian based geometrically nonlinear formulation of the Kirchhoff-Love shell element. The element formulation for linear analysis is deduced from the nonlinear one by introducing the assumption of small displacements and deformation, thus neglecting the change in structural configuration. Since a review of this shell element derivation is rather space-demanding, only the most important element formulae are given below. An interested reader is referred to [16] where the topic is covered extensively.

The shell mid-surface in the initial configuration is given by a parametric function: $\mathbf{x}=\mathbf{x}(\xi_1, \xi_2)$, where ξ_1, ξ_2 are the parametric coordinates (Fig. 2).

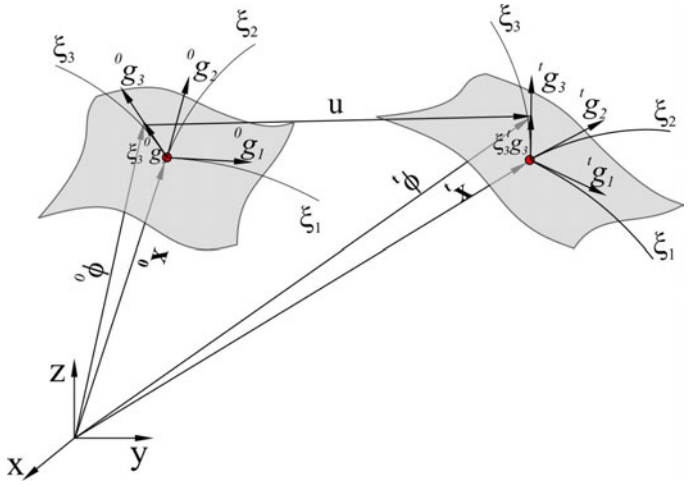

Fig. 2 Initial and deformed shell mid-surface

The position vector of an arbitrary point of the shell is given by the following equation:

$$\boldsymbol{\varphi}\left(\xi_1,\xi_2,\xi_3\right)=\mathbf{x}\left(\xi_1,\xi_2\right)+\xi_3\mathbf{g}_3 \quad \text{with} \quad \left(-t/2\right)\le\xi_3\le\left(t/2\right), \tag{7}$$

where t denotes the shell thickness and ξ_3 is the parametric coordinate corresponding to the thickness direction. The covariant base vectors in the reference configuration are obtained from the derivatives of the position vector with respect to the curvilinear coordinates, as follows:

$$\mathbf{g}_\alpha=\mathbf{x}_{,\alpha} \text{ for } \alpha=1,2\,. \tag{8}$$

The cross product of basic vectors $\mathbf{g}_1$ and $\mathbf{g}_2$ yields the director (vector of surface normal):

$$\mathbf{g}_3 = \frac{\mathbf{g}_1 \times \mathbf{g}_2}{\left|\mathbf{g}_1 \times \mathbf{g}_2\right|}. \tag{9}$$

After discretization of the displacement field and computation of the displacement first order derivatives, one can define the typical Kirchhoff-Love shell strain field consisting of the membrane and flexural parts. The corresponding membrane and flexural strain-displacement matrices are given in the following form, respectively:

$$\mathbf{B}_I^m = \begin{bmatrix} R^I_{,1}\mathbf{g}_1 \cdot \mathbf{e}_1 & R^I_{,1}\mathbf{g}_1 \cdot \mathbf{e}_2 & R^I_{,1}\mathbf{g}_1 \cdot \mathbf{e}_3 \\ R^I_{,2}\mathbf{g}_2 \cdot \mathbf{e}_1 & R^I_{,2}\mathbf{g}_2 \cdot \mathbf{e}_2 & R^I_{,2}\mathbf{g}_2 \cdot \mathbf{e}_3 \\ \left(R^I_{,1}\mathbf{g}_2 + R^I_{,2}\mathbf{g}_1\right)\cdot \mathbf{e}_1 & \left(R^I_{,1}\mathbf{g}_2 + R^I_{,2}\mathbf{g}_1\right)\cdot \mathbf{e}_2 & \left(R^I_{,1}\mathbf{g}_2 + R^I_{,2}\mathbf{g}_1\right)\cdot \mathbf{e}_3 \end{bmatrix}, \tag{10}$$

$$\mathbf{B}_I^b = \begin{bmatrix} \mathbf{B}_1^{bI}\cdot \mathbf{e}_1 & \mathbf{B}_1^{bI}\cdot \mathbf{e}_2 & \mathbf{B}_1^{bI}\cdot \mathbf{e}_3 \\ \mathbf{B}_2^{bI}\cdot \mathbf{e}_1 & \mathbf{B}_2^{bI}\cdot \mathbf{e}_2 & \mathbf{B}_2^{bI}\cdot \mathbf{e}_3 \\ \mathbf{B}_3^{bI}\cdot \mathbf{e}_1 & \mathbf{B}_3^{bI}\cdot \mathbf{e}_2 & \mathbf{B}_3^{bI}\cdot \mathbf{e}_3 \end{bmatrix}, \tag{11}$$

where $\mathbf{e}_1$, $\mathbf{e}_2$, $\mathbf{e}_3$ are the basis vectors of the global coordinate system, $R^I_{,1}$ and $R^I_{,2}$ are the NURBS first order derivatives with respect to the curvilinear coordinates, while the components of flexural strain-displacements matrix are computed as follows:

$$\mathbf{B}_1^{bI} = -R^I_{,11}\mathbf{g}_3 + \frac{1}{\sqrt{\bar{j}}}\left[R^I_{,1}\mathbf{g}_{1,1}\times\mathbf{g}_2 + R^I_{,2}\mathbf{g}_1\times\mathbf{g}_{1,1}\right] + \frac{\mathbf{g}_3\times\mathbf{g}_{1,1}}{\sqrt{\bar{j}}}\left[R^I_{,1}\mathbf{g}_2\times\mathbf{g}_3 + R^I_{,2}\mathbf{g}_3\times\mathbf{g}_1\right],$$

$$\mathbf{B}_2^{bI} = -R^I_{,22}\mathbf{g}_3 + \frac{1}{\sqrt{\bar{j}}}\left[R^I_{,1}\mathbf{g}_{2,2}\times\mathbf{g}_2 + R^I_{,2}\mathbf{g}_1\times\mathbf{g}_{2,2}\right] + \frac{\mathbf{g}_3\times\mathbf{g}_{2,2}}{\sqrt{\bar{j}}}\left[R^I_{,1}\mathbf{g}_2\times\mathbf{g}_3 + R^I_{,2}\mathbf{g}_3\times\mathbf{g}_1\right], \tag{12}$$

$$\mathbf{B}_3^{bI} = -R^I_{,12}\mathbf{g}_3 + \frac{1}{\sqrt{\bar{j}}}\left[R^I_{,1}\mathbf{g}_{1,2}\times\mathbf{g}_2 + R^I_{,2}\mathbf{g}_1\times\mathbf{g}_{1,2}\right] + \frac{\mathbf{g}_3\times\mathbf{g}_{1,2}}{\sqrt{\bar{j}}}\left[R^I_{,1}\mathbf{g}_2\times\mathbf{g}_3 + R^I_{,2}\mathbf{g}_3\times\mathbf{g}_1\right],$$

where $\bar{j}$ is the intensity of the cross product $\mathbf{g}_1\times\mathbf{g}_2$, $R^I_{,11}$, $R^I_{,22}$ and $R^I_{,12}$ are the NURBS second order derivatives with respect to the curvilinear coordinates and $\mathbf{g}_{i,j}$ represents the first order derivative of the basic vector $\mathbf{g}_i$ with respect to the curvilinear coordinate j.

Introducing the above given matrices into the principle of virtual work, one obtains the variation of strain energy as:

$$\delta W^{\text{int}} = \delta\mathbf{u}_i^T \int_\Omega \left[t\left(\mathbf{B}_i^m\right)^T \mathbf{D}\mathbf{B}_j^m + \frac{t^3}{12}\left(\mathbf{B}_i^b\right)^T \mathbf{D}\mathbf{B}_j^b \right] d\Omega\, \mathbf{u_j}, \tag{13}$$

and, hence, the element stiffness matrix in the following form:

$$\mathbf{K}_{IJ} = \int_{\Omega_e} \left[t\left(\mathbf{B}_I^m\right)^T \mathbf{D}\mathbf{B}_J^m + \frac{t^3}{12}\left(\mathbf{B}_I^b\right)^T \mathbf{D}\mathbf{B}_J^b \right] d\Omega, \tag{14}$$

where $\mathbf{D}$ is the constitutive tensor of the isotropic material transformed to the covariant basis:

$$\mathbf{D}=\frac{E}{\left(1-\nu^2\right)}\begin{bmatrix}\left(\mathbf{a}_0{}^{11}\right)^2 & \nu\mathbf{a}_0{}^{11}\mathbf{a}_0{}^{22}+\left(1-\nu\right)\left(\mathbf{a}_0{}^{12}\right)^2 & \mathbf{a}_0{}^{11}\mathbf{a}_0{}^{12} \\ & \left(\mathbf{a}_0{}^{22}\right)^2 & \mathbf{a}_0{}^{22}\mathbf{a}_0{}^{12} \\ \textit{symmetric} & & 0.5\cdot\left[\left(1-\nu\right)\mathbf{a}_0{}^{11}\mathbf{a}_0{}^{22}-\left(1-\nu\right)\left(\mathbf{a}_0{}^{12}\right)^2\right]\end{bmatrix}, \tag{15}$$

where E is Young's modulus, ν Poisson's ratio and $\mathbf{a}_0{}^{ij}$ are the components of the contravariant basis [16].

4. Single patch problem

The academic example of the cylinder quarter depicted in Fig. 3, left, is considered first to demonstrate the isogeometric FEM analysis by means of the presented shell formulation using a single patch. The geometry of the cylinder is defined by the radius of 1 m, length of 1 m and thickness of 0.02 m. It is made of steel (Young's modulus 2e11 N/m^2 and the Poisson coefficient 0.3). As shown in Fig. 3 left, one straight edge of the structure is clamped, while the other straight edge is exposed to the uniform transverse edge load of 1N/m. Since rotations are not directly available as the degrees of freedom, the realization of the clamped boundary condition is required to fix translations in three rows (Fig. 3, middle), whereby the distance between the rows corresponds to the shell thickness. Fig. 3, right, gives the contour plot for the displacement in the z-direction.

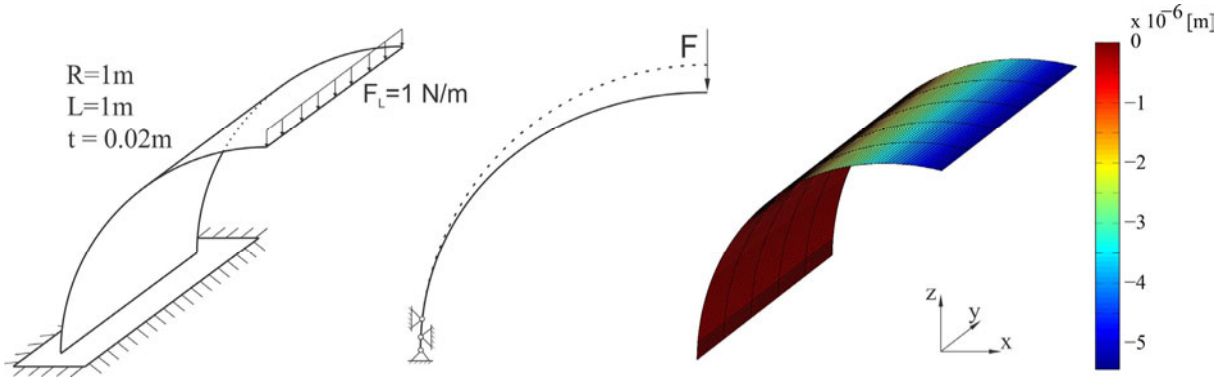

Fig. 3 Model of the cylinder quarter, realization of clamped boundary conditions and contour plot for the displacement in z-direction

The convergence analysis performed for different degrees of the NURBS and the FE mesh is summarized in Fig. 4 which gives the displacement of the loaded edge in the z-direction. The FE mesh refinement has been carried out by increasing the number of elements along the cylinder arc. Obviously, the results with different degrees of NURBS converge to the same solution and, as expected, the models with higher degree NURBS converge faster. The converged result obtained by means of classical FEM involved 100 quadratic CQUAD8 shell elements from the NXNastran element library along the cylinder arc. It should be emphasized that the CQUAD elements implement the Mindlin-Reissner kinematics. The converged results obtained by both approaches show very good agreement.

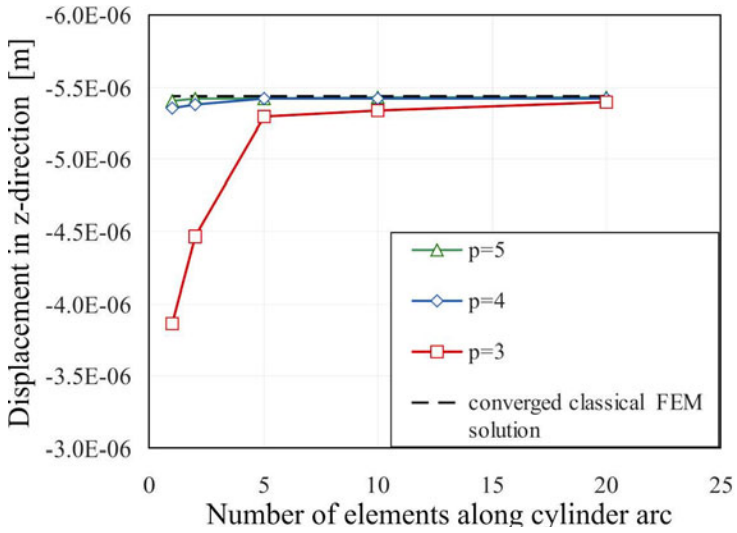

Fig. 4 Result convergence analysis of NURBS-based FEM models with different order of basic functions

5. Multi patch problem with bending strips

Complex structures often cannot be modelled by a single patch. While a simple interconnection of two patches (just a merging line, or a curve) provides the continuity of translations, it does not provide the continuity of rotations and therewith the continuity of bending moments between the patches. A simple idea on how to cope with the problem implies the introduction of an additional small patch into a narrow interconnection zone (Fig. 5) with the aim of adequate transfer of bending moments between the two patches.

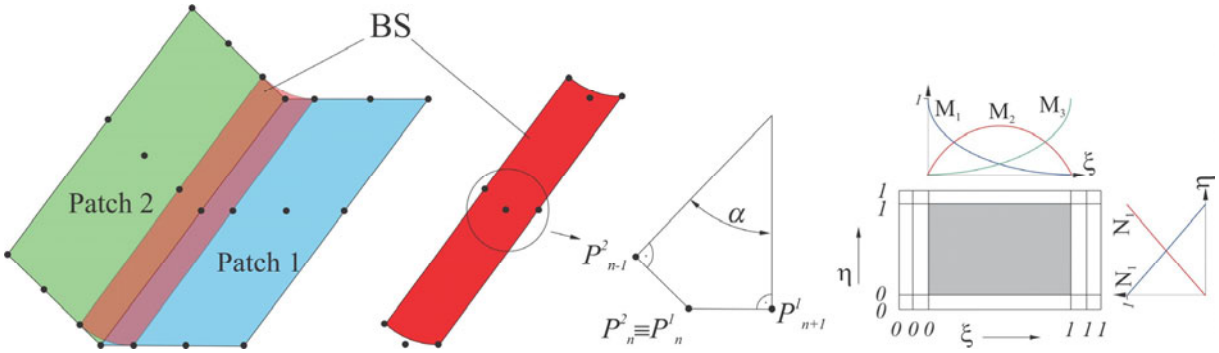

Fig. 5 The bending strip (BS) approach for the interconnection of two patches – strip geometry and the minimum requirement from the basic functions

As can be seen in Fig. 5, left and middle, the two patches (Patch 1 and Patch 2) merge along the line defined by the control polygon points $P^1_{n,i}$ (belonging to Patch 1) and $P^2_{n,j}$ (belonging to Patch 2). To provide an adequate geometric merging of the patches, it is necessary that the polygon control points defining the merging line (or curve, in general) are identical.

The additional patch, denoted as 'bending strip' (BS), needs to be defined by NURBS, whose degree is at least two because of the second order derivative required by the strain-displacement matrix. The simplest suitable form for the bending strip is a cylinder-like section, and three points suffice to determine the curvature (Fig. 5, middle). This further requires knot insertion on both patches to be connected, whereby the knots are inserted at a rather small distance from the merging line. Hence, the polygon control points $P^1_{n-1,i}$ and $P^2_{n+1,j}$ are additionally defined on the patches 1 and 2, respectively (Fig. 5, left and middle). Weight coefficients equal to one are assigned to the edge points of the elements. The weight

coefficients of points $P^1_{n-1,i}$ and $P^2_{n+1,j}$, are determined based on the angle formed between these points, which is given by the scalar product:

$$\alpha = \arccos\left(\frac{\left(P^1_{n-1}P^1_n\right)\cdot\left(P^1_nP^2_{n+1}\right)}{\left|P^1_{n-1}P^1_n\right|\cdot\left|P^1_nP^2_{n+1}\right|} \right). \tag{16}$$

The basic problem in defining the bending strip is how to determine its bending stiffness in order to assure adequate bending moment transfer between the patches. Because the bending strip width is small (approximately the thickness of structural elements), the stiffness of the strip needs to be greater compared to the stiffness of the modelled structures. In contrast to the definition of Kirchhoff's shell, only the part of the stiffness matrix related to bending is computed for the bending strips:

$$\mathbf{K}^{(e)} = \int_{\Omega_e} \left[\left(\mathbf{B}^b_e\right)^T \frac{t^3}{12} \mathbf{D}_s \mathbf{B}^b_e \right] d\Omega \,. \tag{17}$$

Also, the description of the bending strip material is adequately modified so that Hooke's matrix reads:

$$\mathbf{D}_s = \begin{bmatrix} E_s & 0 & 0 \\ 0 & 0 & 0 \\ 0 & 0 & 0 \end{bmatrix}, \tag{18}$$

with modified Young's modulus *Es* that is at least 2 orders of magnitude greater than the one of the actual structural material, whereby too high values of E_S which would make the global stiffness matrix ill-conditioned are avoided. Such a design of the material constitutive matrix ensures that the bending strips only penalize the change in the angle during the deformation between the triples of control points at the patch interface [17].

6. Isogeometric analysis of the excavator boom

The application of the developed numerical tools is also to be demonstrated on actual structures encountered in engineering practice. In this specific case, it is the excavator boom, whose CAD model is shown in Fig. 6.

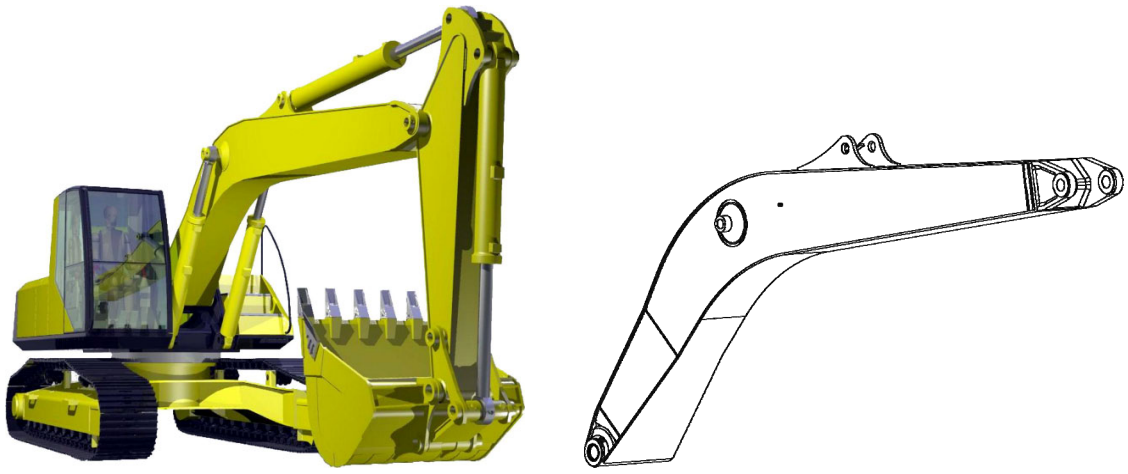

Fig. 6 CAD model of the excavator and its boom

The kinematical boundary conditions and loads shown in Fig. 7 are primarily chosen for the purpose of demonstration of the developed numerical tools, although the force values and directions are realistic for the considered machinery. Three FEM models have been developed. The first two FEM models are the NURBS-based multi-patch models, while the third one is the classical FEM model (Lagrangian shape functions) using CQUAD elements from NXNastran.

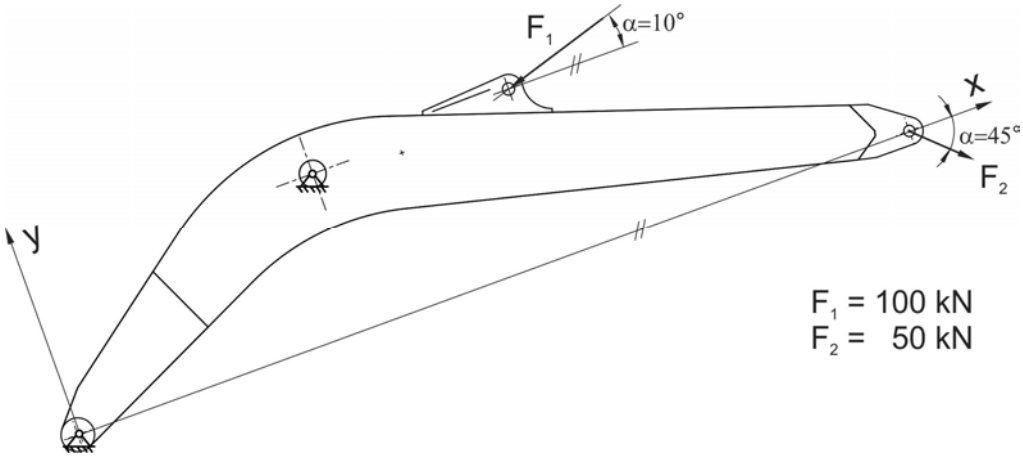

Fig. 7 Big arm of the excavator with boundary conditions and loads

Each of the NURBS-based multi-patch FEM models consists of 87 patches with 8 different shell sections (different thickness). They both use NURBS of the same order with the degree of basic functions in both directions equal to 3. Actually, the only difference between the NURBS-based FEM models is in the number of elements, Fig. 8. The number of elements differs in only one direction. Such mesh refinement has been carried out in order to better capture the bending in vertical plane. The NURBS-based FEM model with a coarser mesh has 4 elements in most patches in both directions, i.e. 16 elements per patch, 12 of which are used for the bending strips. Hence, most of the patches are essentially discretized by 4 (2×2) elements and the mesh can be described as coarse. But since the basic functions of the third order have been used, the obtained results are of good quality. The finer NURBS-based FEM model is obtained by inserting 2 elements into the height direction of the boom (i.e. only over the side walls). The number of degrees of freedom in the model with the coarse NURBS-based FEM mesh is 9363 and with the finer mesh, it is 10323.

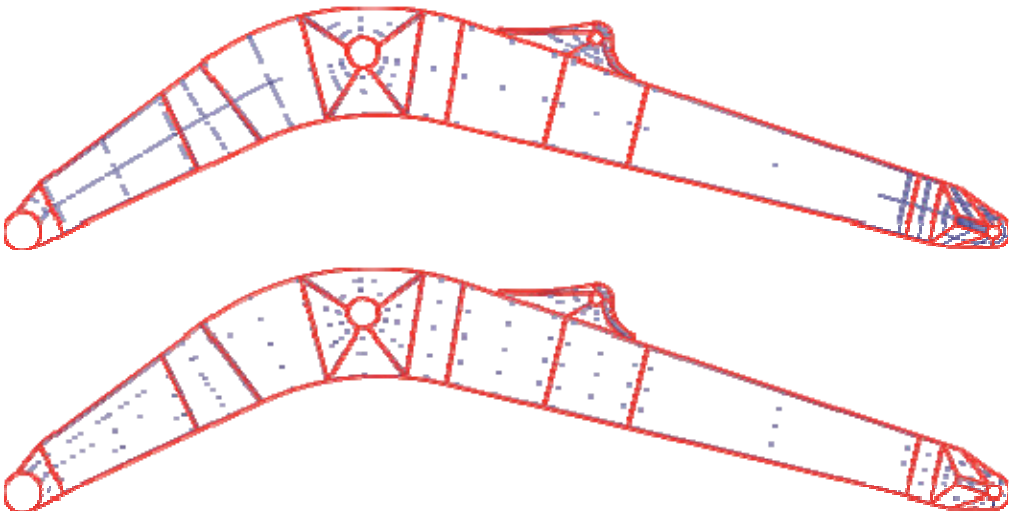

Fig. 8 Multi patch NURBS-based FEM models with a coarse mesh and a finer mesh

A comparison of the maximal displacement magnitude predicted by the three models is given in Table 1. A direct solver has been used with both models. Regarding accuracy, the results by the NURBS-based FEM and classical FEM models are in good agreement. It can be noted that the NURBS-based results converge to a slightly less stiff solution (approximately by 2%), which is to be attributed to different formulations of the applied elements (Mindlin-Reissner with classical FEM and Kirchhoff-Love with NURBS-based elements) in combination with a relatively high ratio of the structure length (more than 5 m) to thickness (between 1 and 1.5 cm).

Table 1 NURBS-based and classical FEM results

FEM model	Number of DOF	Maximal displacement magnitude [m]	Relative difference to classical FEM [%]
NURBS I	9363	$3.1287 \cdot 10^{-3}$	5.00
NURBS II	10323	$3.3599 \cdot 10^{-3}$	2.02
Classical FEM	65478	$3.2934 \cdot 10^{-3}$	-

The contour plot in Fig. 9 gives the displacements magnitude for the finer NURBS-based FEM model.

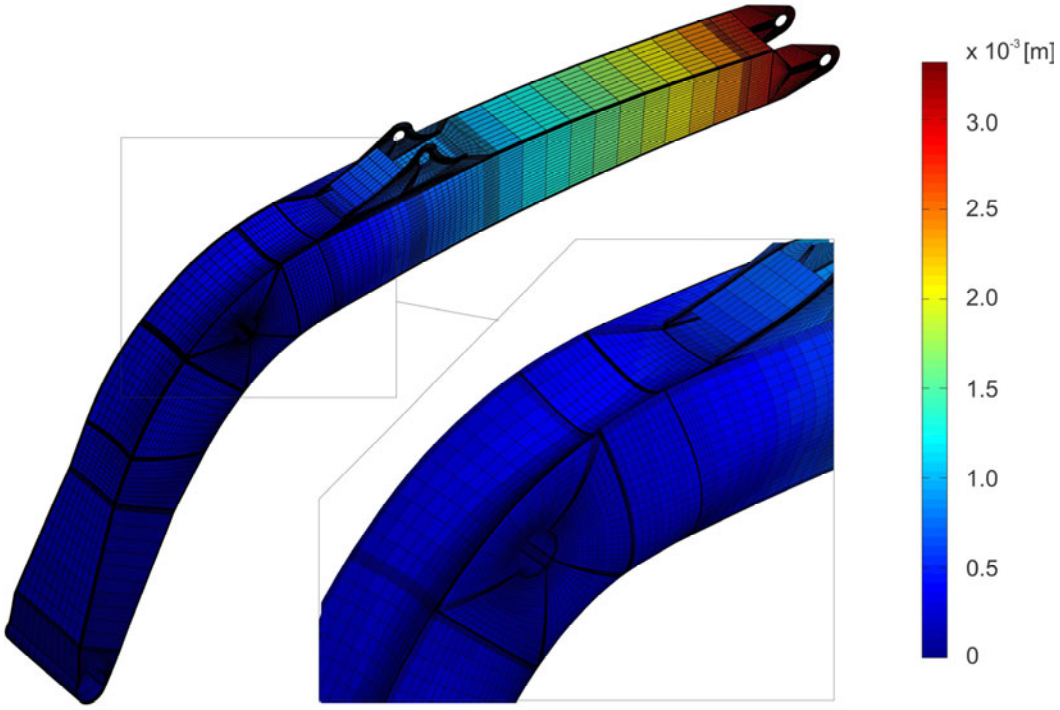

Fig. 9 Contour plot for displacement magnitude obtained by the finer NURBS-based FEM model

7. Conclusions

The isogeometric FEM analysis is a relatively new direction of the FEM development in the field of structural analysis. It has drawn significant attention in the recent years and the theoretical background is already well established. Practical advantages of the NURBS-based approach are still to be demonstrated and well documented through its application to engineering structures. This paper offers a contribution in this direction by considering the boom structure of an excavator.

The obvious advantage offered by the NURBS-based FEM is in the fact that the CAD models already use NURBS to describe complex geometries. Hence, the presented approach enables seamless integration between CAD and FEM. An advantage offered by the Kirchhoff-Love shell formulation is related to the size of the system of equations to be solved. This is a consequence of the fact that there are only translations as the degrees of freedom (no rotations). The dynamic analysis would particularly benefit from this advantage. However, it comes together with the limitation that only rather thin structures can be adequately modelled. The influence of transverse shear effects is expected to be especially noticeable when the dynamic behaviour with higher vibrational mode shapes is involved. Furthermore, more complex geometries require the multi-patch approach together with bending strips for their adequate coupling. Although this approach yields good results, it is accompanied by a numerical effect one needs to be aware of. Namely, the method requires the insertion of additional control polygon points, which increases the size of the model. Additionally, the bandwidth of the stiffness matrix may get noticeably larger, which further deteriorates the numerical efficiency if a direct solver is used for the computation. Node re-numbering may be required in such a case. Alternatively, an iterative solver may be used.

REFERENCES

[1] Hughes T.J.R., Cottrell J.A., Bazilevs Y., *Isogeometric analysis: CAD, finite elements, NURBS, exact geometry and mesh refinement*. Computer Methods in Applied Mechanics and Engineering, Vol. 194, Issues 39–41, 2005, pp. 4135–4195.

[2] Kiendl J., Bletzinger K.-U., Linhard J., Wüchner R., *Isogeometric shell analysis with Kirchhoff–Love elements*, Computer Methods in Applied Mechanics and Engineering, Vol. 198, Issues 49-52, 2009, pp. 3902-3914.

[3] Benson D.J., Bazilevs Y., Hsu M.C., Hughes T.J.R., *Isogeometric shell analysis: The Reissner–Mindlin shell*, Computer Methods in Applied Mechanics and Engineering, Vol. 199, Issues 5-8, 2010, pp. 276-289.

[4] Ahmad S., Irons B. M., Zienkiewicz O. C., *Analysis of thick and thin shell structures by curved finite elements*, International journal for numerical methods in engineering, Vol. 2, 1970, pp. 419-451.

[5] Bischoff M., Ramm E., *Shear deformation elements for large strains and rotations*, International Journal for Numerical Methods in Engineering, Vol. 40, Issue 23, 1997, pp. 4427-4449.

[6] Gruttmann F., Wagner W., *A linear quadrilateral shell element with fast stiffness computation*, Computer Methods in Applied Mechanics and Engineering, Vol. 194, Issues 39-41, 2005, pp. 4279-4300.

[7] Marinković D., Köppe H., Gabbert U., *Degenerated shell element for geometrically nonlinear analysis of thin-walled piezoelectric active structures*, Smart Materials and Structures, Vol. 17, Issue 1, 2008, 015030.1-10.

[8] Prathap G., *The finite element method in structural mechanics*, Kluwer Academic Publishers, Netherlands, 1993.

[9] Bucalem M. L., Bathe K. J., *Finite element analysis of shell structures*, Archives of Computational Methods in Engineering, Vol. 4, Issue 1, 1997, pp. 3-61.

[10] Milić P., Marinković D., *Isogeometric structural analysis based on NURBS shape functions*, Facta Universitatis, Series: Mechanical Engineering, Vol. 11, Issue 2, 2013, pp. 193-202.

[11] Carl de Boor, *On calculating with B-Splines*, Journal of approximation theory, Vol. 6, Issue 1, 1972, pp. 40-62.

[12] Piegl L. A., W. Tiller, *The NURBS Book*, Springer, 1996.

[13] Rogers D. F., *An Introduction to NURBS with Historical Perspective*, Academic Press, 2001.

[14] Kirchhoff G. R, *Uber das Gleichgewicht und Bewegungen einer elastischen Scheibe*, J. Reine u. Angew. Math. 40, 1850, pp. 51-88

[15] Love A. E. H., *On the small free vibrations and deformations of elastic shells*, Philosophical trans. of the Royal Society (London), Série A, Vol. 179, 1888, pp. 491–549.

[16] Nguyen-Thanha N., Valizadehb N., Nguyenc M.N., Nguyen-Xuand H., Zhuange X., Areiasf P., Zih G., Bazilevsg Y., Lorenzisa De L., Rabczukb T., *An extended isogeometric thin shell analysis based on Kirchhoff–Love theory*, Computer Methods in Applied Mechanics and Engineering, Vol. 284, 2015, pp. 265-291.

[17] Kiendl J., Bazilevs Y., Hsu M.-C., Wüchner R., Bletzinger K.-U., *The bending strip method for isogeometric analysis of Kirchhoff–Love shell structures comprised of multiple patches*, Computer Methods in Applied Mechanics and Engineering, Vol. 199, Issues 37-40, 2010, pp. 2403-2416.

Submitted: 09.6.2014

Accepted: 04.3.2015

Predrag Milić
Faculty of Mechanical Engineering
University of Niš, A. Medvedeva 14, Niš, Serbia
Dragan Marinković
Department of Structural Analysis, Berlin Institute of Technology, Strasse des 17. Juni 135, Berlin, Germany
Faculty of Mechanical Engineering
University of Niš, A. Medvedeva 14, Niš, Serbia